



HAL
open science

Same Not the Same Thermally Driven Transformation of Nickel Phosphinate-Bipyridine One-Dimensional Chains into Three-Dimensional Coordination Polymers

A. Guerri, M. Taddei, T. Bataille, S. Moneti, M.-E. Boulon, C. Sangregorio, F. Costantino, A. Ienco

► **To cite this version:**

A. Guerri, M. Taddei, T. Bataille, S. Moneti, M.-E. Boulon, et al.. Same Not the Same Thermally Driven Transformation of Nickel Phosphinate-Bipyridine One-Dimensional Chains into Three-Dimensional Coordination Polymers. *Crystal Growth & Design*, 2018, 18 (4), pp.2234-2242. 10.1021/acs.cgd.7b01672 . hal-01774413

HAL Id: hal-01774413

<https://univ-rennes.hal.science/hal-01774413>

Submitted on 14 May 2018

HAL is a multi-disciplinary open access archive for the deposit and dissemination of scientific research documents, whether they are published or not. The documents may come from teaching and research institutions in France or abroad, or from public or private research centers.

L'archive ouverte pluridisciplinaire **HAL**, est destinée au dépôt et à la diffusion de documents scientifiques de niveau recherche, publiés ou non, émanant des établissements d'enseignement et de recherche français ou étrangers, des laboratoires publics ou privés.

Same not the Same: Thermally-Driven Transformation of Nickel Phosphinate-Bipyridine 1D Chains into 3D Coordination Polymers

Annalisa Guerri[§], Marco Taddei[‡], Thierry Bataille[†], Simonetta Moneti[‡], Marie-Emmanuelle Boulon[§], Claudio Sangregorio^{‡,§}, Ferdinando Costantino^{‡,‡*} and Andrea Ienco^{‡*}

[§] Dipartimento di Chimica, University of Florence, Via della Lastruccia 3, I-50019, Sesto Fiorentino, Firenze, Italy

[‡] Energy Safety Research Institute, Swansea University – Bay Campus, Fabian Way, Swansea, SA1 8EN, United Kingdom

[†] Sciences Chimiques de Rennes (UMR 6226), CNRS, Université de Rennes 1, Avenue du General Leclerc, 35042 Rennes Cedex, France

[‡] Consiglio Nazionale delle Ricerche - Istituto di Chimica dei Composti Organo Metallici (CNR-ICCOM) Via Madonna del Piano 10, I-50019 Sesto Fiorentino (Firenze), Italy.

[‡] Department of Chemistry, Biology and Biotechnologies, University of Perugia, Via Elce di Sotto, 8-06124, Perugia, Italy.

Keywords: Coordination polymers, Metal phosphinates, Phase transitions, Non-ambient diffraction

ABSTRACT

Three 1D nickel coordination polymers (CPs) based on P,P'-diphenylethylenediphosphinic acid and three different bis-pyridine co-ligands, namely 4,4'-bipyridine (bipy), 1,2-bis(4-pyridyl)ethane (bpy-ane) and 1,2-bis(4-pyridyl)ethane (bpy-ene), were prepared in mild hydrothermal conditions from water solutions containing the dissolved reagents. The CPs have formula $[\text{Ni}(\text{H}_2\text{O})_4(\text{bipy})\cdot\text{pc}_2\text{p}]_n$ (**1**), $[\text{Ni}(\text{H}_2\text{O})_4(\text{bpy-ane})\cdot\text{pc}_2\text{p}]_n$ (**2**), and $[\text{Ni}(\text{H}_2\text{O})_4(\text{bpy-ene})\cdot\text{pc}_2\text{p}]_n$ (**3**) and their structural features were investigated by single crystal X-ray diffraction, UV-VIS, FT-IR spectroscopies and magnetic measurements. They are constituted of infinite $\text{Ni}(\text{H}_2\text{O})_4(\text{bis-pyridine})$ 1D rows connected, through hydrogen bonds, with the phosphinic acids placed among adjacent rows. Although the formulas and the structural topologies of the three compounds are almost identical, they behave in different manners upon heating. Compound **1** yields an amorphous phase when water molecules are thermally removed, whereas compound **3** undergoes interesting phase transformations derived from the connection of Ni atoms with the phosphinates oxygen atoms, increasing the dimensionality to 3D and maintaining crystallinity. The behavior of compound **2** has some analogies to that of **3** although a complete structural characterization was not performed because of a significant crystallinity loss of the heated phase. The structural features were studied by means of combination of variable temperature (VT) single crystal and powder X-ray diffraction and thermogravimetric analysis. The reason for these different behaviors was ascribed to both the length and the flexibility degree of the nitrogenated co-ligands.

INTRODUCTION

Chemistry is about transformations. The large majority of chemical reactions are carried out in liquid media, being the molecules free of moving around and to assume conformations favorable to the reactions to take place.¹ Metal-organic frameworks (MOFs), and coordination polymers (CPs) in general, are classes of compounds that can easily show structural transformations at the solid state driven by external stimuli, such as light, pressure and heat.²⁻⁴ The majority of the structural changes can be ascribed either to a modification of ligand conformation or to the removal of solvent molecules, usually placed in voids or in channels as crystallization solvent. Less frequently, the formation or breakage of some bonds are also events taking place upon external stimuli and they can occur through crystal-to-crystal or crystal-to-amorphous phase transformations. Understanding the factors that influence the structural transformations in these classes of solids is crucial to gain the ability to design new and more efficient materials.⁵ Crystal-to-crystal transformation induced by the loss of crystallization water or other solvents is a typical reaction already observed in several compounds.⁶⁻⁸ However, the majority of CPs or MOFs described in the literature exhibits reversible solvent loss and/or uptake, without changes in dimensionality: in other words, no strong bonds which increase the dimensionality are formed upon solvent loss. The reversibility of this event in flexible CPs, associated with structural transformation due to changes in ligand conformation, is typically called breathing effect. A large number of MOFs and CPs reported in literature shows this phenomenon.⁹⁻¹³ Systems with change of dimensionality of the system are rare to the best of our knowledge.^{2-3, 14-18} On the contrary, CPs based on diphosphinate ligands (see chart 1) frequently show structural modifications induced by the temperature, leading also to changes of the dimensionality of the network.¹⁹⁻²² Diphosphinate linkers feature some chemical and geometrical similarities with carboxylate and phosphonate moieties (see chart 2). Diphosphinates have the advantage of being versatile in tuning the electronic and steric properties of the organic residues attached to the phosphorus atom.

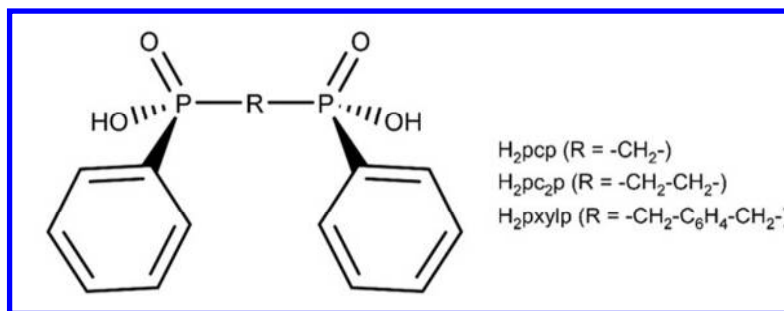


Chart 1. Molecular structure of a diphenyl-bisphosphinate with different substituting groups.

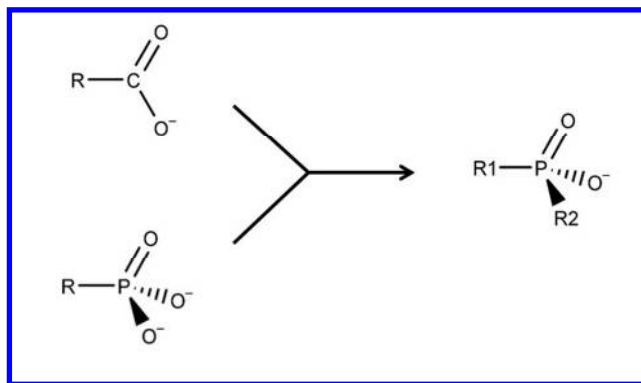
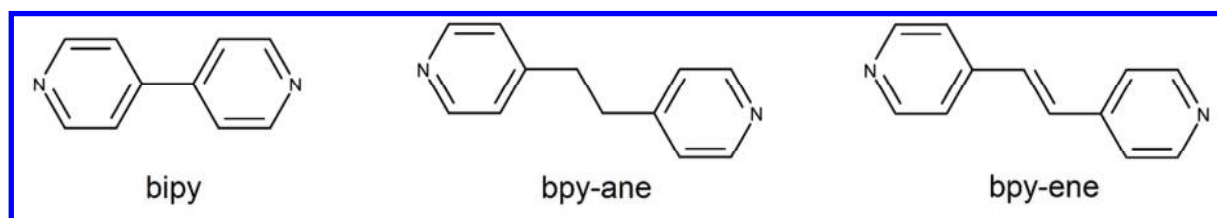


Chart 2. Structural relationships among carboxylates, phosphonates and phosphinates.

As an example, the 3D network $[\text{Cu}(\text{pc}_2\text{p})(\text{bipy})(\text{H}_2\text{O})\cdot 2.5\text{H}_2\text{O}]_n$ (where $\text{H}_2\text{pc}_2\text{p} = \text{P},\text{P}'$ -diphenylethylenediphosphinic acid, $\text{bipy} = 4,4'$ -bipyridine) converted in different crystalline phases when heated up to 120°C . Differently, in solution, it transformed into a 2D grid $[\text{Cu}(\text{pc}_2\text{p})(\text{bipy})(\text{H}_2\text{O})\cdot 3\text{H}_2\text{O}]_n$, showing a rare example of modification from 3D to 2D network.²³ Moreover, by heating the iso-topological 2D grid $[\text{Cu}(\text{pxylp})(\text{bipy})(\text{H}_2\text{O})_2\cdot 2\text{H}_2\text{O}]_n$ (where $\text{H}_2\text{pxylp} = \text{P},\text{P}'$ -diphenyl-*p*-xylylenediphosphinic acid), the 3D network $[\text{Cu}(\text{pxylp})(\text{bipy})]_n$ was obtained.²⁴ Finally, the metal-organic nanotubes (MONTs) having formula $[\text{Cu}(\text{pcp})(\text{bipy})\cdot 5\text{H}_2\text{O}]_n$ and $[\text{Cu}(\text{pcp})(\text{bpy-ane})\cdot 2.5\text{H}_2\text{O}]_n$ [where $\text{H}_2\text{pcp} = \text{P},\text{P}'$ -diphenylmethylenediphosphinic acid, $\text{bpy-ane} = 1,2$ -bis(4-pyridyl)ethane] displayed a very particular behavior: by heating the crystals up to 250°C , the water molecules were removed from the cavity but the framework remained unchanged.^{25,26} Above this temperature, the compounds started to decompose. On the contrary, when the crystal of MONT with bpy-ane was heated in water at 90°C for 30 days, the compound transformed into a 1D compound of formula $[\text{Cu}(\text{pcp})(\text{bpy-ane})(\text{H}_2\text{O})]_n$, a structural isomer without voids. In the same conditions, the analogous MONT with bipy remained unchanged. The reason of this behavior was attributed to the non-existence of a stable 1D phase for the latter due to a predicted thermodynamically unfavorable crystal packing.²⁷ Herein, we report on the structural transformations observed in a novel class of nickel phosphinates containing bipyridine co-ligands. By adding together Ni and pc_2p with the three co-ligands showed in chart 3, namely bipy , bpy-ane and 1,2-bis(4-pyridyl)ethylene (bpy-ene), we obtained 1D coordination polymers of general formula $[\text{Ni}(\text{H}_2\text{O})_4(\text{bis-pyridine})\cdot \text{pc}_2\text{p}]_n$ and with similar crystal arrangement constituted by cationic 1D chains of $[\text{Ni}(\text{H}_2\text{O})_4(\text{bis-pyridine})]^{2+}$. The polymers with bpy-ane and bpy-ene maintain an ordered crystal arrangement after heating and they undergo a crystal-to-crystal transformation into a 3D coordination network. The study of these transformations sheds some light on the mechanism of network formation in different but related systems, such as the $\text{M}(\text{II})$, pcp , bis-pyridines and the $\text{M}(\text{II})$, pc_2p , bis-pyridines.

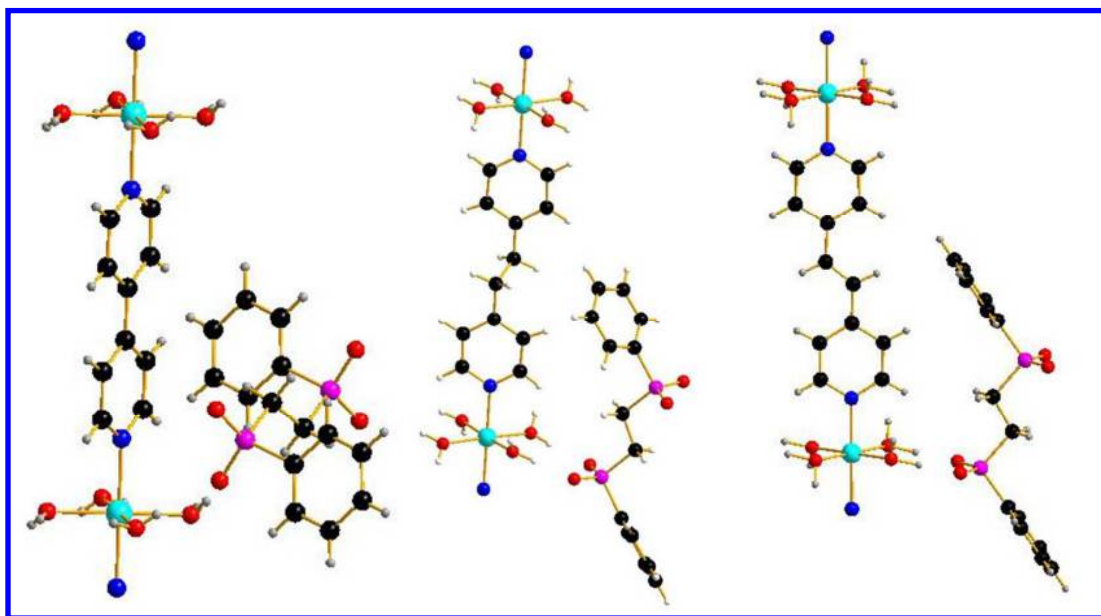


7
8
9
10
11
12
13
14
15
16
17
18
19
20
21
22
23
24
25
26
27
28
29

Chart 3. Structure of the nitrogenated co-ligands used in this work.

RESULTS AND DISCUSSION

Green crystals of $[\text{Ni}(\text{H}_2\text{O})_4(\text{bipy})\cdot\text{pc}_2\text{p}]_n$ (hereafter **1**), $[\text{Ni}(\text{H}_2\text{O})_4(\text{bpy-ane})\cdot\text{pc}_2\text{p}]_n$ (hereafter **2**) and $[\text{Ni}(\text{H}_2\text{O})_4(\text{bpy-ene})\cdot\text{pc}_2\text{p}]_n$ (hereafter **3**) were obtained by mixing in water nickel acetate, $\text{H}_2\text{pc}_2\text{p}$ and bipy (**1**) or bpy-ane (**2**) or bpy-ene (**3**) at 90°C . Crystal structures of the three compounds were determined by single crystal X-ray diffraction analysis (Figure 1). All the structures are constituted of cationic 1D chains of $[\text{Ni}(\text{H}_2\text{O})_4(\text{L})]_n^{2+}$ and dianionic diphosphate moieties. This arrangement, formed by a 1D string of metal, water and bis-pyridine intercalated by another anionic ligand, is relatively common in literature and most of the reported structures were obtained as side products in the attempt to synthesize 3D networks.²⁸⁻⁵⁰ The three compounds reported here are not isostructural and the space groups are different, as reported in table 1. The calculated density for **1** (1.547 g/dm^3) is larger than those of **2** (1.421 g/dm^3) and **3** (1.415 g/dm^3).



49
50
51
52
53
54
55
56
57
58
59
60

Figure 1. Fragment of the structures of **1** (left), **2** (center) and **3** (right).

Table 1. Crystal data and structure refinement for $[\text{Ni}(\text{H}_2\text{O})_4(\text{bipy})\cdot\text{pc}_2\text{p}]_n$, **1**, $[\text{Ni}(\text{H}_2\text{O})_4(\text{bpy-ane})\cdot\text{pc}_2\text{p}]_n$, **2**, $[\text{Ni}(\text{H}_2\text{O})_4(\text{bpy-ene})\cdot\text{pc}_2\text{p}]_n$, **3** and $[\text{Ni}(\text{H}_2\text{O})(\text{bpy-ene})(\text{pc}_2\text{p})]_n$, **3a**

Identification code	1	2	3	3a
Empirical formula	C24 H30 N2 Ni O8 P2	C26 H34 N2 Ni O8 P2	C26 H32 N2 Ni O8 P2	C52 H44 N4 Ni2 O10 P4
Formula weight	595.15	623.20	621.18	1126.21
Temperature (K)	293(2)	100(2)	173(2)	173(2)
Wavelength (Å)	0.71069	1.54184	0.71069	0.71069
Crystal System	Triclinic	Monoclinic	Monoclinic	Monoclinic
Space Group	P -1	C2/c	C2/m	C2/c
Unit Cell Dimensions (Å, °)	a=7.196 (1) b=9.841(3) c=10.381(2) α =63.70(2) β =75.86(2) γ =81.99(2)	a = 11.5588(3) b = 9.4672(2) c = 27.3181(6) β = 102.907(2)	a = 11.5550(9) b = 9.4320(9) c = 13.6180(10) β = 100.701(8)	a = 25.6156(8) b = 9.4288(3) c = 21.3284(8) β = 94.458(4)
Volume (Å ³)	638.7(3)	2913.9(1)	1458.4(2)	5135.7(3)
Z	1	4	2	4
Density (calculated) (g/cm ³)	1.547	1.421	1.415	1.457
Absorption coefficient (mm ⁻¹)	0.937	2.424	0.824	0.920
F(000)	310	1304	648	2320
Crystal size (mm)	0.570 x 0.100 x 0.100	0.2 x 0.1 x 0.08	0.45 x 0.15 x 0.15	0.2 x 0.2 x 0.15
Theta range for data collection (°)	2.236 to 24.970	6.093 to 72.262	4.369 to 28.890	4.265 to 29.328
Index ranges	0 ≤ h ≤ 8, -11 ≤ k ≤ 11, -11 ≤ l ≤ 12	-13 ≤ h ≤ 14, -11 ≤ k ≤ 8, -33 ≤ l ≤ 33	-11 ≤ h ≤ 15, -11 ≤ k ≤ 11, -18 ≤ l ≤ 17	-32 ≤ h ≤ 29, -12 ≤ k ≤ 9, -28 ≤ l ≤ 29
Reflections collected	2441	15787	3436	12104
Independent reflections	2246 [R(int) = 0.0231]	2858 [R(int) = 0.0464]	1775 [R(int) = 0.0462]	5871 [R(int) = 0.0356]
Completeness	96.4 % (to theta = 25.240°)	99.8 % (to theta = 67.684°)	98.9 % (to theta = 25.000°)	98.8 % (to theta = 25.240°)
Refinement method	Full-matrix least-squares on F ²	Full-matrix least-squares on F ²	Full-matrix least-squares on F ²	Full-matrix least-squares on F ²
Data / restraints / parameters	2246 / 0 / 185	2858 / 0 / 245	1775 / 0 / 107	5871 / 0 / 306
Goodness-of-fit on F ²	1.071	1.075	0.965	0.947
Final R indices [I > 2σ(I)]	R1 = 0.0290, wR2 = 0.0699	R1 = 0.0382, wR2 = 0.0874	R1 = 0.0446, wR2 = 0.0951	R1 = 0.0588, wR2 = 0.1568
R indices (all data)	R1 = 0.0397, wR2 = 0.0737	R1 = 0.0516, wR2 = 0.0952	R1 = 0.0756, wR2 = 0.1008	R1 = 0.0972, wR2 = 0.1703

In all cases, Ni(II) metal atom is octahedrally coordinated by four water molecules and by two nitrogen atoms belonging to two different bis-pyridine ligands. The Ni-O and Ni-N distances are comparable in the three compounds (see Table S1, ESI). The conformation of pc₂p can be defined using the C_{ipso}-P-P-C_{ipso} dihedral angle where C_{ipso} is the carbon atom of the phenyl ring bonded to the phosphorus atom.

The value of the angle is about 180° for all the structures. This value is one of the most recurrent in the pc_2p complexes reported up to now.⁵¹ Strong hydrogen bonds, with O-O distances in the range 2.64-2.76Å, exist between the water molecules and the oxygen atoms of the pc_2p . The $Ni(H_2O)_4$ groups are surrounded by four pc_2p anions and the oxygen atoms of the pc_2p are connected with four different $Ni(H_2O)_4$ moieties. The H-bond network in **1** is different with respect to **2** and **3**, as shown in Figure S1. Therefore, the whole supramolecular arrangement is different and it is schematically illustrated in Figure 2. The pc_2p group is represented by a purple cylinder while the $[Ni(H_2O)_4(bis-pyridine)]_n$ column is schematized by a line formed by green cubes and light blue parallelepipeds. In **2** and **3**, the cylinders and the cubes are arranged as in a chessboard, while in **1** the pc_2p are intercalated between the lines of the $[Ni(H_2O)_4(bis-pyridine)]_n$ columns.

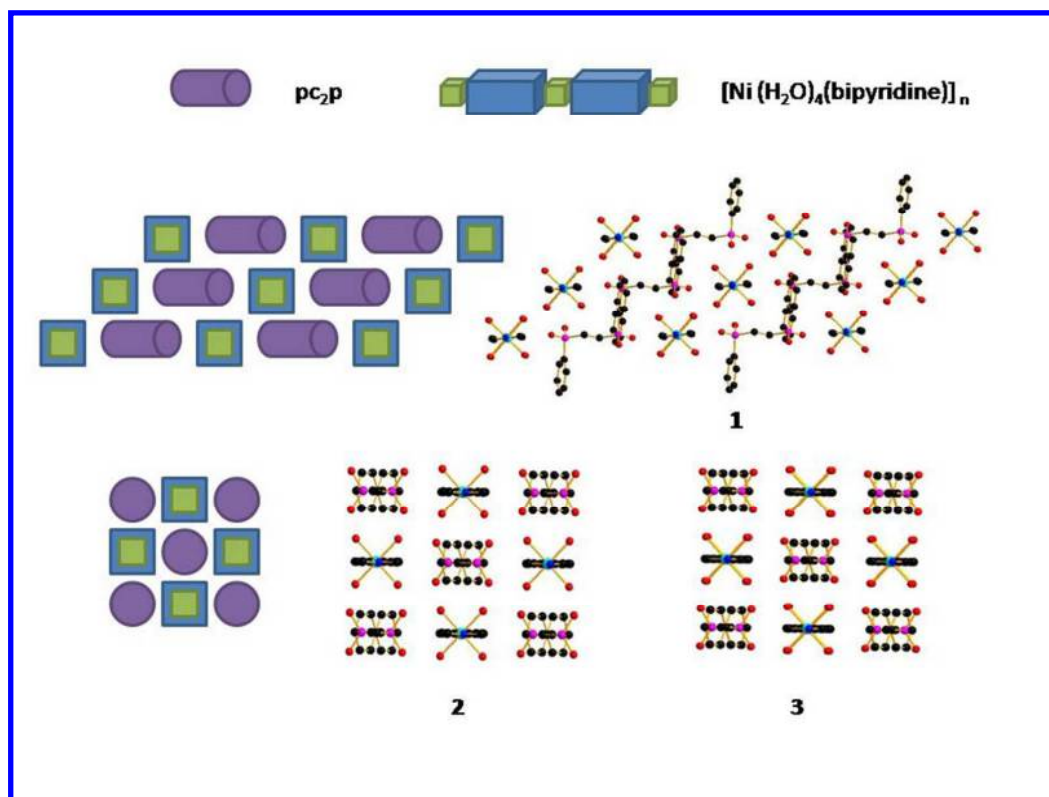


Figure 2. Schematic representation of the crystal packing for **1**, **2** and **3**. Purple cylinders represent pc_2p groups; green cubes ($Ni(H_2O)_4$) and light blue parallelepipeds (bis-pyridine) are used to visualize the $[Ni(H_2O)_4(bis-pyridine)]_n$ columns.

We expected that crystal structures **1-3** were good candidates for solid state transformations driven by temperature. The phosphinate moiety decomposes at around 300°C , a temperature comparable to thermally stable carboxylate based MOFs. We have also previously observed that the coordination polymers formed by bis-pyridines and phosphinates are generally crystalline and stable up to the decomposition temperature of bis-pyridines (250°C).²³⁻²⁶ Thermogravimetric analysis (TGA) of **1** shows

1 that the phase is stable up to 150°C (see Figure S2). The observed weight loss of 37.6% (35.8 Calcd.)
2 corresponds to the release of the four water molecules and the degradation of the bipy. Between 270°C
3 and 450°C, the diagram shows a new stability range that most likely corresponds to $[\text{Ni}(\text{pc}_2\text{p})]_n$ phase.
4 The temperature dependent X-ray diffraction (TD-XRD) experiment (see Figure S3) shows that **1** is
5 stable and crystalline up to 150°C. At higher temperature, only few broad peaks are observed and they
6 are attributed to the $[\text{Ni}(\text{pc}_2\text{p})]_n$ phase. In the case of **2**, as shown in Figure 3a, the synthesized phase is
7 stable up to 90°C. The weight loss between 90°C and 140°C corresponds to the removal of four water
8 molecules (exp. 11.0%, calcd 11.6%). The successive loss corresponds to the burning of the bis-pyridine
9 ligand (exp. 39.2; calcd. 41.1). The TD-XRD analysis between room temperature and 100°C (see Figure
10 3c) confirms the results of the TGA, i.e. the anhydrous $[\text{Ni}(\text{bpy-ene})(\text{pc}_2\text{p})]_n$ phase, **2b**, is a crystalline
11 phase. In addition, it is relatively stable at room temperature, as additional peaks of the pristine
12 compound are only seen after 17 hours in ambient conditions. Such behavior allowed us to readily
13 stabilize **2b** to collect high-resolution powder X-ray diffraction (PXRD) data at 110 °C. Powder pattern
14 indexing led to unit cell dimensions close to their precursor's, i.e., $a = 10.656(8) \text{ \AA}$, $b = 12.941(8) \text{ \AA}$, $c =$
15 $26.22(1) \text{ \AA}$, $\beta = 94.52(6)^\circ$, $V = 3604.8 \text{ \AA}^3$ [$M_{17} = 11.2$, $F_{17} = 27(0.107, 60)$], probable space group P
16 $2/m$. This result suggests that the full dehydration does not modify drastically the crystal structure of **2**,
17 and the schematic arrangement of entities could obviously be preserved as illustrated in Figure 2. More
18 on the possible structure of **2b** will be discussed below. The TGA of **3** is reported in Figure 3b. There is
19 no significant weight loss up to 90°C. In the range 90°C – 120°C, the corresponding weight losses
20 match with the removal of three water molecules (exp. 8.9%, Calcd 8.7%). Between 140°C and 160°C,
21 also the fourth water molecule is lost (exp. 2.7%, Calcd 2.9%). The anhydrous phase is stable up to
22 200°C. The additional weight loss corresponds to the removal of the bipyridine at higher temperature.
23 Finally, the $[\text{Ni}(\text{pc}_2\text{p})]_n$ phase is stable up to 450°C. A TD-XRD experiment, performed at a much lower
24 heating rate up to 160 °C, allowed to observe the corresponding dehydration stages at lower
25 temperatures, as shown in figure 3d. The $[\text{Ni}(\text{H}_2\text{O})(\text{bpy-ene})(\text{pc}_2\text{p})]_n$ phase, **3a**, is obtained as a
26 crystalline phase between 60 and 100 °C. It transforms into the crystalline anhydrous $[\text{Ni}(\text{bpy-ene})(\text{pc}_2\text{p})]_n$
27 phase, **3b**, which is observed till the end of the experiment at 160 °C. In this case ab-initio
28 indexing was not possible due to loss of crystallinity and broadening of many peaks. An additional *in*
29 *situ* XRD experiment was performed while cooling the sample in different atmospheres, to evaluate
30 whether **3b** is stable in ambient conditions. This phase seems only sensitive to water, as it rehydrates
31 into its monohydrate parent **3a** in air, while it is stable under pure N_2 (see Figure S3). Additionally,
32 phase **3a** does not convert back into **3** when placed in contact with water.
33
34
35
36
37
38
39
40
41
42
43
44
45
46
47
48
49
50
51
52
53
54
55
56
57
58
59
60

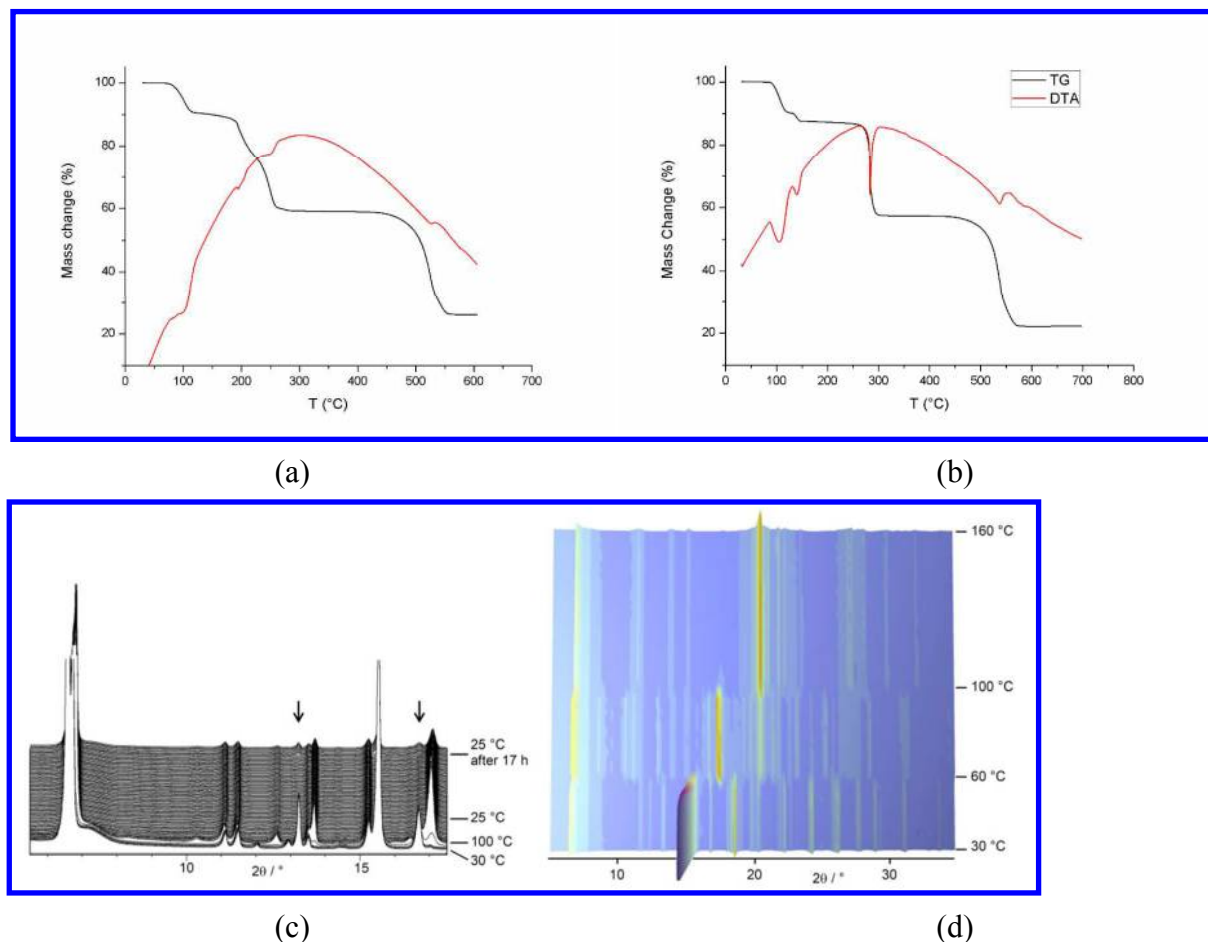


Figure 3: (a) TG/DTA curve of compound **2**; (b) TG/DTA curve of compound **3**; (c) temperature dependent XRD experiment showing the dehydration of **2** and the slow re-hydration of **2b** back to ambient; (d); temperature dependent XRD experiment for **3**.

We tried to dehydrate single crystals of **2** and **3** simply by heating a batch of crystals at 140 °C for one night under vacuum. For **2**, we did not obtain suitable crystals, while for **3** after the treatment, it was possible to collect and solve the structure of **3a** by single crystal X-ray diffraction. As already pointed out, in air **3b** spontaneously rehydrates into its monohydrate parent.

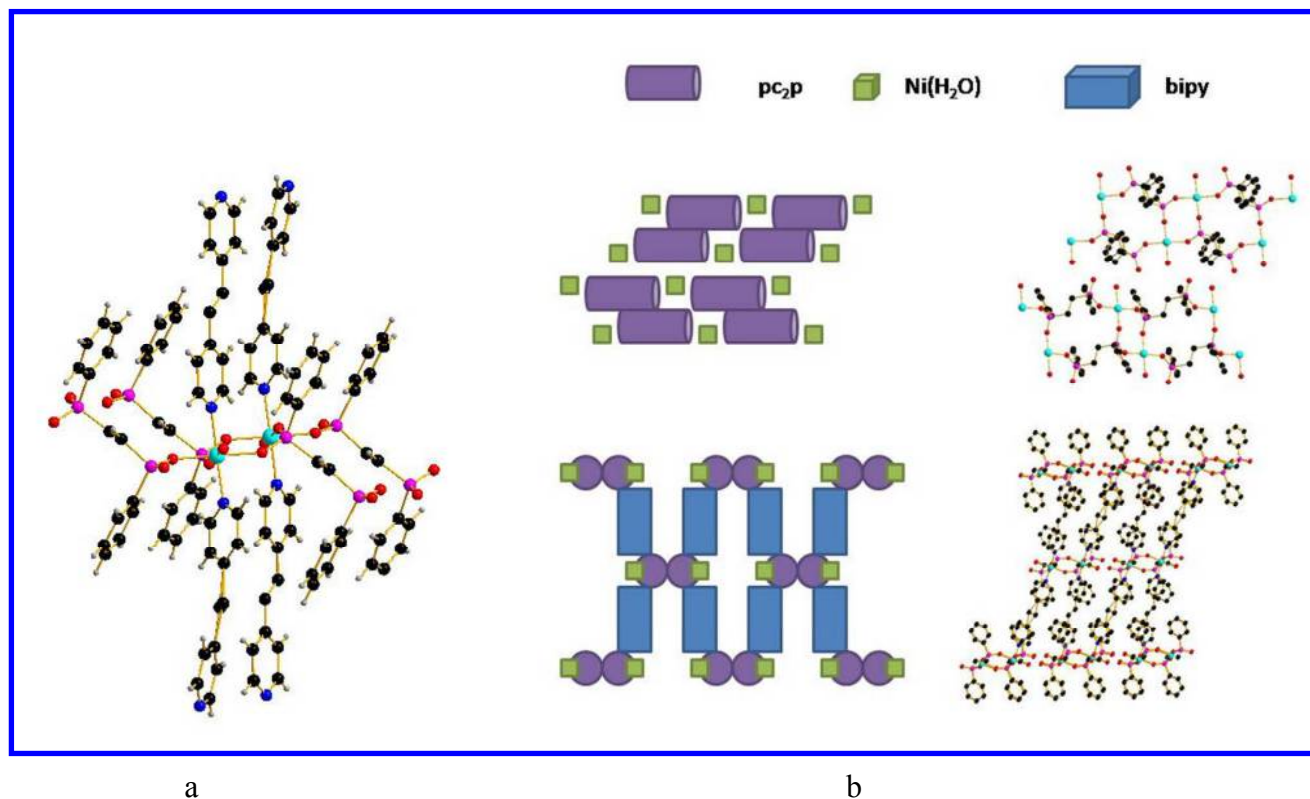


Figure 4. a) Fragment of the structures of **3a** b) Crystal packing of **3a**. In this case, the green square represents the Nickel atom bonded to one water molecule.

In order to schematize the network, the same representation of Figure 2 for pc_2p , $bipy$ and $Ni(H_2O)$ was used, as well as the corresponding stick and ball models (hydrogen atoms are omitted). The 3D network of **3a** is assembled using Ni and pc_2p (phenyl rings are omitted) in 1D sheets; the latter are connected by the bipyridine molecule. $Ni(II)$ is still octahedrally coordinated, but three basal coordination sites are hereby occupied by oxygen atoms of three different pc_2p ligands and the fourth position is taken up by a water molecule (Figure 4a). The 1D pillars of $[Ni(bipy)]$ are now connected by the pc_2p ligand. A new 1D $[Ni(H_2O)(pc_2p)]$ chain is formed, as shown in Figure 4b. Strong hydrogen bonds are formed between the water molecules and the oxygen atoms of the diphosphinate groups not involved in the metal coordination (O-O distances = 2.71 Å). The 1D $[Ni(bpy-ene)]$ pillars connect the 1D $[Nipc_2p]$ chains and the resulting structure is a 3D network with 3-connected (pc_2p ligand) and 5-connected (Nickel atom) nodes. Figure 5 shows the proposed mechanism of formation of **3a**, focusing on the breaking and formation of coordination bonds that involve Ni and pc_2p , modeled upon the crystal structure of **3**: removal of three water molecules from the Ni coordination sphere (Figure 5a to 5b) triggers reorganization of the hydrogen bonds network and every pc_2p molecule coordinates to three different Ni atoms (Figure 5b to 5c), thus leading to twisting of the pc_2p units and formation of the chains of $Ni(pc_2p)$ held together by hydrogen bonds observed in **3a** (Figure 5c to 5d).

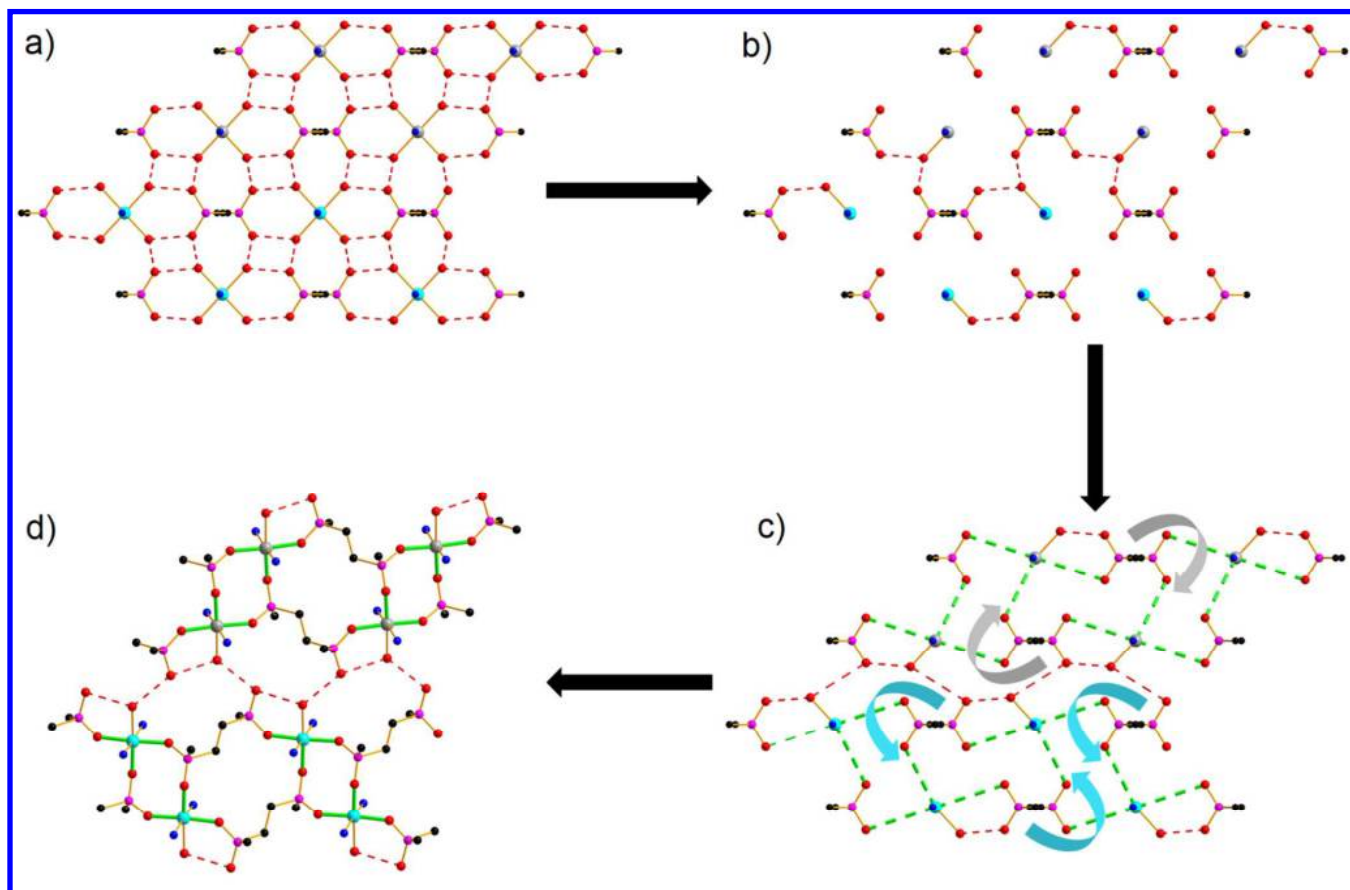


Figure 5. Proposed mechanism for the phase transition leading from **3** to **3a**. (a) Arrangement of Ni octahedra and pc₂p units in **3**. (b) Residual coordination bonds and hydrogen bonds in **3** after removal of three water molecules per Ni atom. (c) Reorganization of hydrogen bonds and formation of new coordination bonds between pc₂p units and Ni atoms, accompanied by twisting of the pc₂p. (d) Final structure of **3a**. Different colors are used to distinguish Ni atoms that end up belonging to different chains in **3a**. Colour code: Ni atoms are represented in light blue and light gray, P atoms are represented in pink, C atoms are represented in black, O atoms are represented in red, N atoms are represented in blue, H atoms are represented in white. Hydrogen bonds are represented as red dashed lines. Newly formed coordination bonds are represented as dashed green lines in (c) and bold green lines in (d).

Substantial reorganization of the π - π stacking interactions network takes place during the phase transition (Figure S4). **1**, **2** and **3** all feature similar π - π stacking interactions between the phenyl rings of adjacent pc₂p units, while bis-pyridines are not involved in any non-covalent interaction. In **3a** this arrangement is disrupted and new interactions involving also bpy-ene are established. The phase transition does not involve breaking and formation of bonds between bpy-ene and Ni, however the [Ni(bpy-ene)] chains experience a significant distortion in **3a** (Figure S5). The topological analysis reveals a 3,5T1 net, reported to be in the first 30 most frequent underline single net.⁵² Considering the

1 hydrogen bond between the uncoordinated oxygen atom of diphosphinate and the water molecule, the
2 overall topology becomes fsc with a 4-connected (pc₂p ligand) and 6-connected (Nickel atom) nodes.
3 This gives us some hints on the structure **3b**. Likely, the uncoordinated oxygen atoms of the phosphinic
4 ligands could displace the coordinated water molecule thus connecting to the Nickel atom and extending
5 the connectivity into a 3D network.
6
7

8 Since it was not possible to obtain the crystallographic structure of **2b**, we decided to investigate its
9 spectroscopic and magnetic properties and to compare them with those of **2** and **3**. UV-VIS spectra of **2**
10 and **2b** (see Figure S7) display similar features except for a blue shift of the peaks for **2b** suggesting a
11 similar coordination geometry in both cases. Unfortunately, no information could be obtained from EPR
12 spectroscopy since compound **2b** is EPR silent from room temperature down to 10 K probably due to an
13 excessive zero field splitting, (ZFS). As a comparison, **2**, **3** and **3a** spectra have also been recorded at
14 room temperature and 10 K. None of them show EPR transition at this frequency. The temperature
15 dependence of the molar susceptibility product with the temperature, $\chi_M T$, for **2**, shown in Figure S8, is
16 consistent with that expected for a Ni (II) ion in an octahedral ligand field⁵³: $\chi_M T$ increases with
17 temperature up to ca. 25 K and then remains constant at 1.39 emu.K.mol⁻¹ up to the highest measured
18 temperatures. For **2b**, the $\chi_M T$ versus T increases with the temperature until reaching a maximum at 5.5
19 K, it then decreases before reaching a constant value of 1.24 emu.K.mol⁻¹ from 50K to room
20 temperature. As a comparison, **3b** was also measured. The thermal variation of its $\chi_M T$ product
21 undergoes a similar behavior with a maximum at 6.5 K. The low temperature maximum can be
22 attributed to a weak ferromagnetic interactions through O-P-O bridges connecting Ni ions in the dimeric
23 units, and to the large ZFS which characterizes Ni ions in octahedral geometry. The similarity of the
24 room temperature $\chi_M T$ values between **2** and **2b** indicates that the octahedral geometry is preserved
25 upon the phase transition. A square planar coordination would result, indeed, in a diamagnetic behavior,
26 so that this hypothesis can be definitely discarded. Moreover, the low temperature behavior of **2b**,
27 identical to **3b**, suggests a similar metal environment in the two samples, where the Nickel atoms are
28 surrounded by two nitrogen atoms from the pyridine rings and four oxygen atoms from four different
29 pc₂p ligands.
30
31

32 We have presented a very special case in which quasi-similar CPs behave in very different ways, under
33 the same heating conditions. To summarize, at first glance **1**, **2** and **3** are almost the same compounds,
34 having the same formula, the same coordination environment around the Ni metal atom and forming the
35 same 1D network. A closer look reveals a different supramolecular arrangement for **1**, **2** and **3** as well as
36 a different calculated density. The change in behavior could be ascribed to the different length of the
37 bridging unit of the two pyridine molecules. The N-N distances are 7.112(3), 9.390(2) and 9.436(4) Å
38
39
40
41
42
43
44
45
46
47
48
49
50
51
52
53
54
55
56
57
58
59
60

1 for bipy, bpy-ane and bpy-ene in **1**, **2**, and **3**, respectively. The two latter values have to be compared
2 with the equivalent distances of phosphorus atoms of two pc₂p in **2** and **3**, i.e., 9.799(2) Å and 9.855(2)
3 Å respectively. With this in mind, bipy is clearly too short to allow the crystal arrangement shown by **3a**
4 or the expected one for **2b** and **3b**. The identification of the partially hydrated phase **3a** could be related
5 to the different flexibility of bpy-ane and bpy-ene. Bpy-ene preferably adopts a planar conformation,
6 owing to the conjugation of the two pyridine rings through the double bond. In **3a**, one of the
7 crystallographically independent bpy-ene units is already significantly distorted and it is likely that **3b**
8 demands even more distortion. This suggests that the system prefers to retain one water molecule
9 coordinated to each Ni atom instead than replacing it with a P-O group from a phosphinate unit. As a
10 matter of fact, **3b** readily uptakes one water molecule when exposed to moist air, while **3a** is stable over
11 a long period in the presence of water. In the case of **2**, the ideal monohydrate phase **2a** was probably
12 not isolated because the higher flexibility of bpy-ane molecule leads to preferential stabilization of
13 compound **2b**.

14 These findings help us to critically review other transformations observed in previous papers such as the
15 transformation of the 1D MONT compound in 1D strip.²⁷ In that example, the phosphinic ligand (pcp)
16 was linked to copper forming [Cu(pcp)]_n 1D columns. These columns remained stable during the
17 transformation while Cu-N bonds were broken and reformed. In the present work, we observed that the
18 [Ni(bis-pyridine)]_n columns remained the same while new Ni-O bonds were formed in the process. This
19 behavior could be related both to the different strength of the metal-ligand bonds in the two series of
20 compound but also the better chelating ability of pcp, compared to pc₂p, could have a certain importance
21 in the building up well stable [Cu(pcp)]_n columns.

22 Conclusions

23 In this paper, the structure and reactivity of three related 1D Ni-phosphinate CPs were studied. For the
24 three compounds, we have reported how the transformation of 1D coordination compounds in 3D ones
25 induced by the temperature took place. The different mechanisms involved in the formation of the 3D
26 coordination polymers in the case of two related class of ligand which differ only by a methylene group
27 (namely the pcp and the pc₂p ligands) were discussed. We found that pcp reacts first with the metallic
28 center and after the formation of a corner-like polymer the connection among the bipys occurred. In the
29 case of pc₂p, we have found that the affinity of the latter ligand is lower than the one of the bipys. In this
30 way, infinite 1D chains formed by [M(bipy)]_n are present in solution and the pc₂p connect them to build
31 the tridimensional structures. We can say that structures **1**, **2** and **3** can be considered a sort of proto-
32 coordination polymers able to afford novel 3D structures upon heating which cannot be obtained by
33
34
35
36
37
38
39
40
41
42
43
44
45
46
47
48
49
50
51
52
53
54
55
56
57
58
59
60

direct synthesis. In our opinion, this study added important features to the comprehension of the chemistry of CPs based on transition metal phosphinates.

Experimental Section

Materials and Methods: All reagents were analytical-grade commercial products and were used without further purification. The p,p' - diphenylmethylenediphosphinic acid (H₂pcp) was prepared as previously described.^{54,55} Elemental analyses (C, H) were performed with an EA 1108 CHNS-O automatic analyzer. Coupled thermogravimetric (TG) and differential thermal analysis (DTA) measurements were performed using a Netzsch STA490C thermoanalyzer under a 20 mL min⁻¹ air flux with a heating rate of 10 C min⁻¹. The IR spectra were recorded on Shimadzu IRAffinity-1S, equipped with MIRacle PIKE ATR. DRS spectra were recorded in the reflectance mode by using an integrating sphere on a Shimadzu UV-Visible Spectrophotometer UV-2600. BaSO₄ as a reference standard. The spectra were converted to the corresponding absorption spectra by using the Kubelka–Munk equation. *In situ* X-ray powder diffraction measurements were performed within an Anton Paar HTK 1200N chamber attached to a Panalytical Empyrean powder diffractometer. (θ–θ Bragg–Brentano geometry) working with the Cu-Kα radiation (λ Kα₁ = 1.5406 Å, λ Kα₂ = 1.5444 Å) selected with a flat multilayer X-ray mirror (Bragg-Brentano HD[®]). Data were collected with a Pixel 1D silicon-strip detector, in the useful angular range. Powder pattern indexing was carried out with the program DICVOL06.⁵⁶

Synthesis of [Ni(H₂O)₄(bipy)·pc₂p]_n,1: A solution of Ni(CH₃COO)₂·4H₂O (35 mg, 0.14mmol) in water (10 ml) was added to a boiling water solution (60ml) of H₂pc₂p (43 mg, 0.14mmol) and bipy (22 mg, 0.14mmol). The resulting solution was boiled till green cubes started separating. Then the mixture was held at ca. 80°C to complete the precipitation of the complex. The compound was filtered, washed with water and dried in air, at room temperature. Yield 68% based on Nickel. Anal. Calc. for C₂₄ H₃₀ Ni O₈ N₂ P₂, mw=595.15gmol⁻¹: C, 48.44; N, 4.71; H, 5.08. Found: C, 48.42; N, 4.69; H, 5.15%.

Synthesis of [Ni(H₂O)₄(bpy-ane)·pc₂p]_n,2: A solution of Ni(CH₃COO)₂·4H₂O (35 mg, 0.14mmol) in water (10 ml) was added to a boiling water solution (60ml) of H₂pc₂p (43 mg, 0.14 mmol) and bpy-ane (26 mg, 0.14mmol). The resulting solution was boiled till green cubes started separating. Then the mixture was held at ca. 80°C to complete the precipitation of the complex. The compound was filtered, washed with water and dried in air, at room temperature. Yield 74% based on Nickel. Anal. Calc. for C₂₆ H₃₄ Ni O₈ N₂ P₂, mw=623.20gmol⁻¹: C, 50.11; N, 4.50; H, 5.50. Found: C, 50.15; N, 4.45; H, 5.57%.

Synthesis of [Ni(H₂O)₄(bpy-ene)·pc₂p]_n,3: A solution of Ni(CH₃COO)₂·4H₂O (35 mg, 0.14mmol) in water (10 ml) was added to a boiling water solution (60ml) of H₂pc₂p (43 mg, 0.14mmol) and bpy-ene

(26 mg, 0.14mmol). The resulting solution was boiled till green cubes started separating. Then the mixture was held at ca. 80°C to complete the precipitation of the complex. The compound was filtered, washed with water and dried in air, at room temperature. Yield 63% based on Nickel. Anal. Calc. for C₂₆H₃₂NiO₈N₂P₂, mw=621.19g mol⁻¹: C, 50.27; N, 4.51 ; H, 5.19. Found: C, 50.30; N, 4.55; H, 5.28%.

X-Ray Structure Determination: The crystal data of compounds **1**, **2**, **3** and **3a** are presented in Table 1. The single-crystal X-ray experiments were carried out on a CCD diffractometer with Mo K_α or Cu K_α radiation. The program CrysAlisCCD⁵⁷ was used for data collection. Data reductions (including absorption corrections) were carried out with the program CrysAlis RED.⁵⁸ The atomic coordinates were obtained by the direct methods in Sir97.⁵⁹ Structure refinements were performed with SHELXL⁶⁰ using the full-matrix least-squares method for all the available F² data. All the non-hydrogen atoms were refined anisotropically.

Magnetic Characterization: Magnetic susceptibility measurements were carried out using a Quantum Design MPMS SQUID magnetometer equipped with a 5 T magnet. Raw data were corrected for the diamagnetic contribution of the sample holder, and the intrinsic diamagnetism of the sample, estimated by Pascal's constants.⁶¹ X-band (9.41GHz) EPR spectroscopic studies on microcrystalline powder samples placed in 4mm diameter quartz tubes were carried out at low temperatures using a Bruker E500 spectrometer equipped with an ESR900 (Oxford Instruments) continuous-flow ⁴He cryostat and a SHQ resonator

ACKNOWLEDGEMENTS

A.I. and T.B. are grateful for the Short Term Mobility Program 2013. M.T. is supported by funding from the European Union's Horizon 2020 research and innovation program under the Marie Skłodowska-Curie grant agreement No 663830. AI acknowledges Mr. Carlo Bartoli for his technical assistance.

AUTHOR INFORMATION

E-mail:

Ferdinando Costantino ferdinando.costantino@unipg.it,

Andrea Ienco andrea.ienco@iccom.cnr.it

Note: The authors declare no competing financial interest.

ASSOCIATED CONTENT

CCDC 1564548-1564551 contain the supplementary crystallographic data for this paper. These data can

be obtained free of charge via www.ccdc.cam.ac.uk/data_request/cif, or by emailing data_request@ccdc.cam.ac.uk, or by contacting The Cambridge Crystallographic Data Centre, 12 Union Road, Cambridge CB2 1EZ, UK; fax: +44 1223 336033.

Supporting information available

The supporting information is available free of charge on the ACS publication website at: DOI xxxx
Crystallographic tables containing structural information, bond lengths and angles for compounds **1**, **2**, **3** and **3a**. TGA analysis for compound **1**. Temperature dependent XRPD patterns for compound **1**. Additional structural figures showing the H-bonds nets and the $\pi - \pi$ stacking for compounds **2** and **3**. IR and UV-VIS spectra are also reported.

REFERENCES

- (1) V. V. Boldyrev, *Reactivity of Solids: Past, Present and Future*, Blackwell Science, Cambridge, **1996**.
- (2) Vittal, J. J.; *Supramolecular structural transformations involving coordination polymers in the solid state* *Coord. Chem. Rev.* **2007**, *251*, 1781-1795.
- (3) Kole, G. K.; Vittal, J. J. *Solid-state reactivity and structural transformations involving coordination polymers.* *Chem. Soc. Rev.* **2013**, *42*, 1755-1775.
- (4) Li, C.-P.; Chen, J.; Liu, C.-S.; Du, M. *Dynamic structural transformations of coordination supramolecular systems upon exogenous stimulation* *Chem. Commun.* **2015**, *51*, 2768-2781.
- (5) Tanaka, K. and Toda, F. *Solvent-Free Organic Synthesis* *Chem. Rev.* **2000**, *100*, 1025-1074.
- (6) Rather B., Zaworotko, M. J. *A 3D metal-organic network, [Cu₂(glutarate)₂(4,4'-bipyridine)]*, that exhibits single-crystal to single-crystal dehydration and rehydration *Chem. Commun.* **2003**, 830-831.
- (7) Sun, H.-L., Yin, D.-D.; Chen, Q., Wang, Z. *Europium Pyrimidine-4,6-dicarboxylate Framework with a Single-Crystal-to-Single-Crystal Transition and a Reversible Dehydration/Rehydration Process* *Inorg. Chem.* **2013**, *52*, 3582-3584.
- (8) Zhang, J.-P.; Lin, Y.-Y.; Zhang, W.-X.; Chen, X.-M. *Temperature- or Guest-Induced Drastic Single-Crystal-to-Single-Crystal Transformations of a Nanoporous Coordination Polymer* *J. Am. Chem. Soc.* **2005**, *127*, 14162-14163.
- (9) Férey, G.; Serre, C. *Large breathing effects in three-dimensional porous hybrid matter: facts, analyses, rules and consequences.* *Chem. Soc. Rev.* **2009**, *38*, 1380-1399.
- (10) Habib, H. A.; Sanchiz, J.; Janiak, C. *Mixed-ligand coordination polymers from 1,2-bis(1,2,4-triazol-4-yl)ethane and benzene-1,3,5-tricarboxylate: Trinuclear nickel or zinc secondary building units for three-dimensional networks with crystal-to-crystal transformation upon dehydration* *Dalton Trans.* **2008**, 1734-1744.

- (11) Volkringer, C.; Loiseau, T.; Guillou, N.; Férey, G.; Elkaïm, E.; Vimont, A. XRD and IR structural investigations of a particular breathing effect in the MOF-type gallium terephthalate MIL-53(Ga) *Dalton Trans.* **2009**, 2241-2249.
- (12) Taddei, M.; Costantino, F.; Ienco, A.; Comotti, A.; Dau, P. V.; Cohen, S. M. Synthesis, breathing, and gas sorption study of the first isorecticular mixed-linker phosphonate based metal-organic frameworks *Chem. Commun.* **2013**, *49*, 1315-1317.
- (13) J.-P. Zhang, P.-Q. Liao, H.-L. Zhou, R.-B. Lin, X.-M. Chen Single-crystal X-ray diffraction studies on structural transformations of porous coordination polymers *Chem. Soc. Rev.*, **2014**, *43*, 5789-5814;
- (14) Sánchez Costa, J.; Rodríguez-Jiménez, S.; Craig, G. A.; Barth, B.; Beavers, C. M.; Teat, S. J. Aromí G. Snapshots of a solid-state transformation: coexistence of three phases trapped in one crystal *J. Am. Chem. Soc.* **2014** *136*, 3869-3874;
- (15) Lee, E.; Kim, Y.; Heo, J.; Park K.-M 3D Metal–Organic Framework Based on a Lower-Rim Acid-Functionalized Calix[4]arene: Crystal-to-Crystal Transformation upon Lattice Solvent Removal *Cryst. Growth Des.* **2015** *15*, 3556-3560;
- (16) Wang, X-P; Chen, W-M; Qi, H; Li, X-Y.; Rajnák, C; Feng, Z.-Y.; Kurmoo, M; Boča, R; Jia, C.-J.; Tung, C.-H.; Sun, D.; Solvent-controlled phase transition of a CoII-organic framework: From achiral to chiral and two to three dimensions. *Chem Eur J* **2017**, *23*, 7990-7996;
- (17) Cao, L.-H.; Wei, Y. -S; Xu, H.; Zang, S.-Q.; Mak. T. C. W. Unveiling the Mechanism of Water-Triggered Diplex Transformation and Correlating the Changes in Structures and Separation Properties *Adv. Funct. Mater.* **2015**, *25*, 6448-6457.
- (18) Vittal; J.J.; Quah, H. S. Engineering solid state structural transformations of metal complexes. *Coord. Chem. Rev.* **2017**, *342*, 1-18.
- (19) Costantino, F.; Ienco, A.; Taddei, M. Tailored Organic-Inorganic Materials (Eds.: E. Brunet, J. L. Colon, A. Clearfield), John Wiley & Sons, **2015**, 193–244;
- (20) Costantino, F.; Ienco, A.; Taddei, M. Non-covalent Interactions in the Synthesis and Design of New Compounds (Eds.: Maharramov, A. M.; Mahmudov, K. T.; Kopylovich, M. N.; Pombeiro, A.J.L.) John Wiley & Sons, **2016**, 163-184.
- (21) Vioux, A.; Le Bideau, J.; Mutin, P. H.; Leclercq, D. Topics in Current Chemistry, Springer-Verlag, Heidelberg, **2004**, 145.
- (22) Carson, I.; Healy, M.R.; Doidge, E.D.; Love, J.B.; Morrison, C.A.; Tasker, P.A. Metal-binding motifs of alkyl and aryl phosphinates; versatile mono and polynucleating ligands *Coord. Chem. Rev.* **2017**, *335*, 150-171.

- (23) Bataille, T.; Costantino, F.; Ienco, A.; Guerri, A.; Marmottini, F.; Midollini, S. A snapshot of a coordination polymer self-assembly process: The crystallization of a metastable 3D network followed by the spontaneous transformation in water to a 2D pseudopolymorphic phase *Chem. Commun.* **2008**, 6381-6383.
- (24) Costantino, F.; Ienco, A.; Midollini, S. Different structural networks determined by variation of the ligand skeleton in copper(II) diphosphinate coordination polymers *Cryst. Growth Des.* **2010**, *10*, 7-10.
- (25) Bataille, T.; Costantino, F.; Lorenzo-Luis, P.; Midollini, S.; Orlandini, A. A new copper(II) tubelike metal-organic framework constructed from P,P'-diphenylmethylenediphosphinic acid and 4,4'-bipyridine: Synthesis, structure, and thermal behavior *Inorg. Chim. Acta* **2008**, *361*, 327-334.
- (26) Bataille, T.; Bracco, S.; Comotti, A.; Costantino, F.; Guerri, A.; Ienco, A.; Marmottini, F. Solvent dependent synthesis of micro- and nano-crystalline phosphinate based 1D tubular MOF: Structure and CO₂ adsorption selectivity *CrystEngComm* **2012**, *14*, 7170-7173.
- (27) Taddei, M.; Ienco, A.; Costantino, F.; Guerri, A.; upramolecular interactions impacting on the water stability of tubular metal-organic frameworks *RSC Adv* **2013**, *3*, 26177-26183.
- (28) Woodward, J.D.; Backov, R.V.; Abboud, K.A.; Talham, D.R. Monomers, chains, ladders, and two-dimensional sheets: Structural diversity in six new compounds of Zn(II) with 4,4'-bipyridine. *Polyhedron* **2006**, *25*, 2605-2615.
- (29) Marinescu, G.; Andruh, M.; Julve, M.; Lloret, F.; Llugar, R.; Uriel, S.; Vaissermann, J. Heteropolymetallic Supramolecular Solid-State Architectures Constructed from [Cr(AA)(C₂O₄)₂]⁻ Tectons, and Sustained by Coordinative, Hydrogen Bond and π-π Stacking Interactions (AA = 2,2'-Bipyridine; 1,10-Phenanthroline) *Cryst. Growth Des.* **2005**, *5*, 261-267.
- (30) Wang, R.; Jiang, F.; Zhou, Y.; Han, L.; Hong, M. Syntheses and characterizations of four mixed-ligand hydrogen bonding supramolecular architectures with different structural motifs *Inorg. Chim. Acta* **2005**, *358*, 545-545.
- (31) Chen, H.-J.; Huaxue, H. Synthesis and crystal structure of poly[Co(4,4'-bpy)(H₂O)₄]SO₄·(4-abaH)₂·3H₂O *Jiegou Huaxue (Chin. J. Struct. Chem.)* **2005**, *24*, 236-240.
- (32) Zhang, L.-P.; Zhu, L.-G. The monodentate 4,4'-bipyridine complex tetra-aqua-bis(4,4'-bipyridine)zinc(II) bis-(4-carboxy-benzene-sulfonate) *Acta Crystallogr. Sect. E: Struct. Rep. Online* **2005**, *E61*, m1768-m1770.
- (33) Dong, H.-L.; Xu, L.; Liu, Q.-Y.; Sang, R.-L. Tetra-aqua-bis(4,4'-bipyridine)copper(II) bis(perchlorate) bipyridine tetra-solvate *Acta Crystallogr. Sect. E: Struct. Rep. Online* **2005**, *E61*, m2340-m2342.

- (34) Gao, J-S.; Hou, G-F.; Yu, Y-H.; Hou, Y-J.; Yan, P-F. catena-Poly[[[tetra-aqua-cobalt(II)]- μ -4,4'-bipyridine- κ^2 N:N'] 1,2-phenyl-enedioxy-diacetate 4,4'-bipyridine hemisolvate dihydrate] *Acta Crystallogr. Sect. E: Struct. Rep. Online* **2006**, E62, m2913-m2915.
- (35) Chen, Z.; Liang, F.; Tang, X.; Chen, M.; Song, L.; Hu, R.Z. Syntheses and Structural Characterization of Two Nitrilotriacetate Cobalt Complexes: [$\{\text{CoK}_2(\text{NTA})(\text{Hmta})(\text{H}_2\text{O})_3\}\text{NO}_3\]_n$ and [$\{\text{Co}(4,4'\text{-bpy})_2(\text{H}_2\text{O})_4\}\{\text{Co}_2(\text{NTA})_2(4,4'\text{-bpy})(\text{H}_2\text{O})_2\}$] *Anorg. Allg. Chem.* **2005**, 631, 3092-3095.
- (36) Liu, Y.; Dou, J-M.; Wang, D-Q.; Li, D-C.; Xu, F.; Zhou, L.; Su, H-J. Syntheses and crystal structures of four new complexes [$\text{Mn}(4,4'\text{-bip})_2(\text{OH}_2)_4(\text{DBA})\cdot 4\text{H}_2\text{O}$] and [$\text{M}(\text{OH}_2)(\text{HDP A})_2\cdot 3\text{H}_2\text{O}$] (M = Mn, Co, Ni) *Jiegou Huaxue (Chin. J. Struct. Chem.)* **2006**, 25, 895-902.
- (37) Tong, M-L.; Lee, H. K.; Chen, X-M.; Huang, R-B.; Mak, T.C.W. A novel three-dimensional triangular organic-inorganic hybrid network self-assembled by mononuclear [$\text{Mn}(4,4'\text{-bipyridine})_2(\text{H}_2\text{O})_4\]^{2+} cations and rich solvate 4,4'-bipyridine molecules through hydrogen-bonding and π - π interactions *J. Chem. Soc. Dalton Trans.* **1999**, 3657-3659.$
- (38) Lei, C.; Mao, J-G.; Sun, Y-Q.; Dong, Z-C. Novel inorganic-organic hybrids based on oxo-bridged $\text{M}_6(\text{M})$ centered octahedral cage *Polyhedron* **2005**, 24,295-303.
- (39) Wei, Y-H.; Tan, A-Z.; Chen, Z-L.; Liang, F-P.; Hu, R-X. Syntheses and Crystal Structures of Supramolecular Compounds [$\text{M}(4,4'\text{-bipy})_2(\text{H}_2\text{O})_4\cdot (4,4'\text{-bipy})_2\cdot (3,5\text{-diaba})_2\cdot 8\text{H}_2\text{O}$] (M=Co, Ni, Cd) *Chin. J. Inorg. Chem.* **2006**, 22, 273-280
- (40) Huo, X-K.; Ma, L-F.; Wang, L-Y.; Fan, Y-T. Synthesis, Crystal Structure and Magnetic Properties of a Manganese Complex with One-dimensional Chain Structure *Chin. J. Inorg. Chem.* **2007**, 23, 401-406.
- (41) Zhang, L-P.; Zhu, L-G. Monodentate function of the 4,4'-bipyridine that systematically occurs in the 4-sulfobenzoate manganese(II) complexes: syntheses, crystal structures, and properties *CrystEngComm* **2006**, 8, 815-826.
- (42) Lu, S-F.; Zhu, Y-B.; Liang, Y-C.; Yu, R-M.; Huang, X-Y.; Sun, F-X. Wu, Q-J.; Huang, Z-X. Synthesis, structural feature and intercluster interaction of a series of compounds containing binuclear molybdenum (tungsten) cluster anion *Acta Chim. Sinica* **2004**, 62, 253-261.
- (43) Wang, X-L.; Qin, C.; Wang, E-B. Polythreading of Infinite 1D Chains into Different Structural Motifs: Two Poly(pseudo-rotaxane) Architectures Constructed by Concomitant Coordinative and Hydrogen Bonds *Cryst. Growth Des.* **2006**, 6, 439-443
- (44) Tao, J.; Huang, R-B.; Zheng, L-S.; S.W. Ng Tetra-aqua-bis(4,4'-bi-pyridine)copper(II) 2,6-naphthalene-di-carboxyl-ate trihydrate *Acta Crystallogr., Sect. E: Struct. Rep. Online* **2003**, E59, m614-m615.

- (45) Paz, F. A. A.; Khimyak, Y.Z.; Klinowski, J. Bis(4,4'-bi-pyridine)-tetra-aqua-cobalt(II) 2,6-naphthalenedi-carboxyl-ate dihydrate *Acta Crystallogr., Sect. E: Struct. Rep. Online* **2003**, E59, m8-m10.
- (46) Wang, Q-W.; Li, X-M.; Han, J. Hydrothermal synthesis, crystal structure and magnetic properties of a cobalt(II) coordination polymer assembled by 4-sulfophthalate and 4,4'-bipyridine *Jiegou Huaxue (Chin. J. Struct. Chem.)* **2006**, 25, 1369-1374
- (47) Zhou, Q-X.; Xu, Q-F.; Lu, J-M.; Xia, X-W. Synthesis and structural characterization of a Ni(II) complex $[\text{Ni}(\text{H}_2\text{O})_4(4,4'\text{-bipy})_2](\text{hca})_2$ *Jiegou Huaxue (Chin. J. Struct. Chem.)* **2006**, 25, 1392 – 1396.
- (48) Zhang, L-P.; Zhu, L-G. catena-Poly[[[tetra-aqua-copper(II)]- μ -4,4'-bipyridine- κ^2 N:N'] 4-sulfonatobenzoate] *Acta Crystallogr., Sect. E: Struct. Rep. Online* **2005**, E61, m1264-m1265
- (49) Xie, H-Z.; Li, Z-F.; Zheng, Y-Q. A new trinuclear cobalt(II) complex: deca-aqua- $1\kappa^3\text{O}, 2\kappa^4\text{O}, 3\kappa^3\text{O}$ -bis-(benzene-1,3,5-tricarboxyl-ato)-1[κ]O,3[κ]O-di- μ -4,4'-bipyridine-1:2 $\kappa^2\text{N}:\text{N}'$;2:3 $\kappa^2\text{N}:\text{N}'$ -di-4,4'-bipyridine-1 κ N,3 κ N-tricobalt(II) 4,4'-bipyridine solvate octa-hydrate *Acta Crystallogr., Sect. C: Cryst. Struct. Commun.* **2007**, 63, m30-m32.
- (50) Williams, P.A.M.; Ferrer, E.G.; Baran, E.J.; Piro, O.E.; Ellena, J.A.; Castellano, E.E. XABSOJ : tetraqua-bis(4,4'-bipyridine)-iron(ii) disaccharinate bis(4,4'-bipyridine) *CCDC 188089: Experimental Crystal Structure Determination* **2014**, doi: 10.5517/cc69qdl.
- (45) Costantino, F.; Ienco, A.; Midollini, S.; Orlandini, A.; Sorace, L.; Vacca, A. Copper(II) complexes with bridging diphosphinates - The effect of the elongation of the aliphatic chain on the structural arrangements around the metal centres *Eur J. Inorg. Chem.* **2008**, 3046-3055.
- (46) Alexandrov, E. V., Blatov, V. A., Kochetkov, A. V; Proserpio, D. M. *CrystEngComm* **2008**, 13, 3947-3958.
- (43) Boudreaux, E. A.; Mulay, L. N. Theory and applications of molecular paramagnetism Eds., Wiley-Interscience, New York, N. Y., 1976.
- (47) Midollini, S.; Lorenzo-Luis, P.; Orlandini, A. Inorganic-organic hybrid materials of p,p'-diphenylmethylenediphosphinic acid (H_2pcp) with magnesium and calcium ions: Synthesis and characterization of $[\text{Mg}(\text{Hpcp})_2]$, $[\text{Mg}(\text{Hpcp})_2(\text{H}_2\text{O})_4]$, $[\text{Mg}(\text{pcp})(\text{H}_2\text{O})_3](\text{H}_2\text{O})$, $[\text{Ca}(\text{Hpcp})_2]$ and $[\text{Ca}(\text{pcp})(\text{H}_2\text{O})]$ complexes *Inorg. Chim. Acta* **2006**, 359, 3275-3282
- (48) Garst, M.E. Alkylation of Phenyl Phosphinic Acid *Synth. Commun.*, **1979**, 9, 261-266.
- (49) Boultif, A; Louër. D. Powder pattern indexing with the dichotomy method *J. Appl. Crystallogr.* **2004**, 37, 724-731.
- (50) CrysAlisCCD, Oxford Diffraction Ltd., Version 1.171.33.41 (release 06-05-2009 CrysAlis171.NET)
- (51) CrysAlisRED, Oxford Diffraction Ltd., Version 1.171.33.41 (release 06-05-2009 CrysAlis171.NET)

1 (52) Altomare, A.; Burla, M.C.; Cavalli, M.; Cascarano, G.L.; Giacovazzo, C.; Gagliardi, A.; Moliterni,
2 A.G.G.; Polidori, G.; Spagna, R. SIR97: a new tool for crystal structure determination and refinement
3
4 *J.Appl.Crystallogr.* **1999**, *32*,115-119.

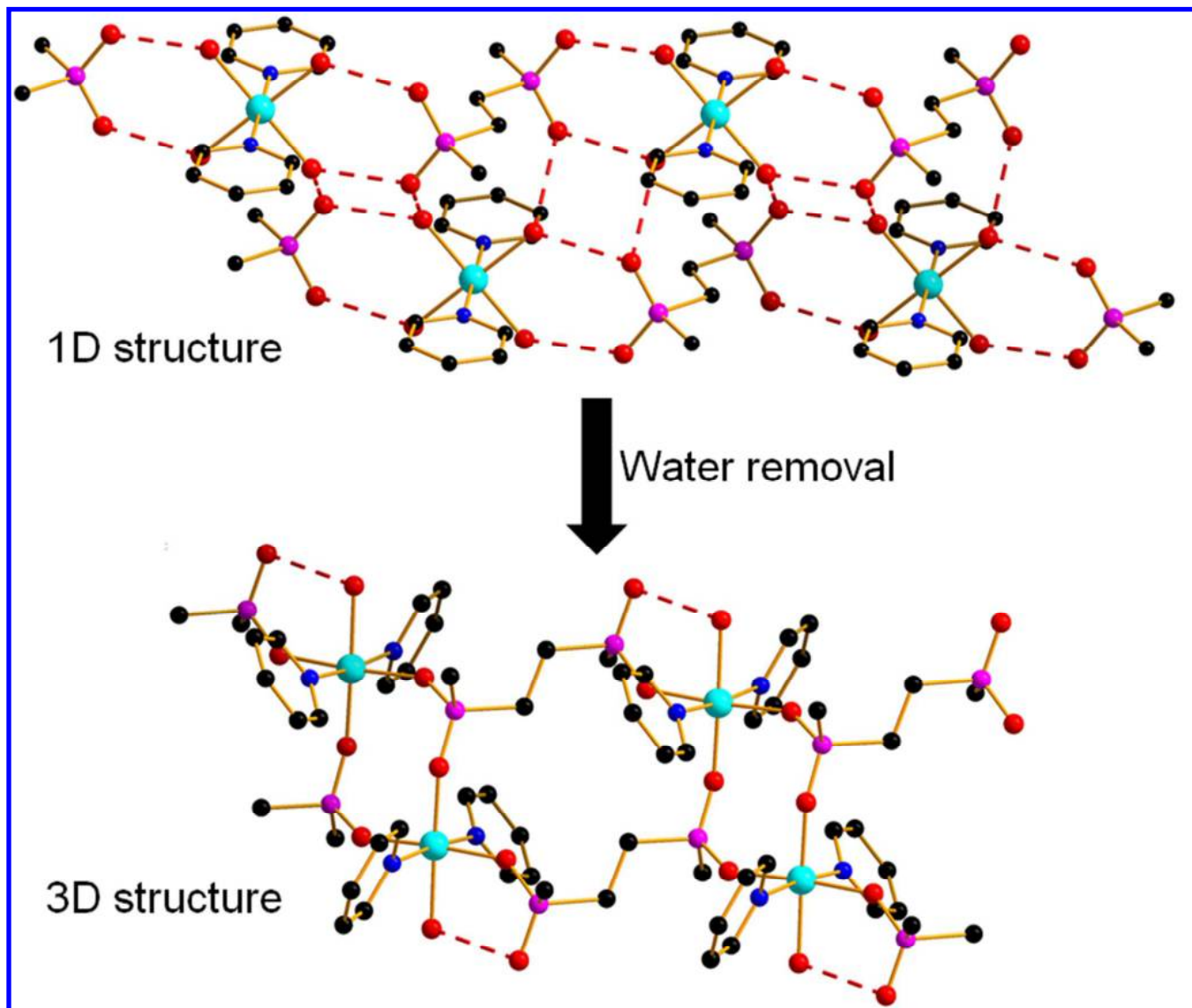
5 (53) Sheldrick, G. M. A short history of SHELX *Acta Crystallogr.* **2008**, *A64*, 112-122.

7 (54) Bain, G. A.; Berry, J. F. Diamagnetic Corrections and Pascal's Constants *J. Chem. Educ.* **2008**, *85*,
8 532-536.
9

For Table of Contents Use Only

Same not the Same: Thermally-Driven Transformation of Nickel Phosphinate-Bipyridine 1D Chains into 3D Coordination Polymers

Annalisa Guerri, Marco Taddei, Thierry Bataille, Simonetta Moneti, Marie-Emmanuelle Boulon, Claudio Sangregorio, Ferdinando Costantino and Andrea Ienco**



Synopsis: Nickel phosphinate-bispyridine 1D chains undergo structural transformation into 3D networks upon heating. The transformation is influenced by the flexibility and the steric hindrance of the co-ligands